

Case Depth and Load Capacity of Case-Carburized Gears

Thomas Tobie, Peter Oster and Bernd-Robert Höhn

Introduction

Compared to non-heat-treated components, case-carburized gears are characterized by a modified strength profile in the case-hardened layer. The design of case-carburized gears is based on defined allowable stress numbers. These allowable stress numbers are valid only for a defined "optimum" case depth. Adequate heat treatment and optimum case depth guarantee maximum strength of tooth flank and tooth root. Variable case depths can lead to a decrease in load capacity. For some applications, including large gears with small modules, maximum load capacity for the tooth flank often cannot be used. Therefore, the optimum case depth is not required. A smaller case depth can meet the load capacity requirement for the actual application without reaching the maximum load capacity and can thereby decrease distortion by hardening and reduce the need for grinding.

For case-carburized gears with adequate case depth, it is generally accepted that pitting cracks are initiated at the surface, where topography of surface and lubricating conditions are important parameters. However, on crack propagation, the stress field of the subsurface region also has an important influence. Furthermore, under special conditions, cracks also can initiate below the surface. The variable stress gradient over depth requires a corresponding gradient of strength. So, to determine an adequate case depth that will ensure pitting resistance, it is essential to know the stress field induced by loading of the tooth flank at the surface, as well as over depth below the surface for all points on the line of contact.

Based on theoretical work and experimental test results, it is planned to introduce an addition to the standardized gear rating according to ISO/DIN (Ref. 2), in which the influence of case depth on load capacity is taken into consideration.

As a gear's tooth flank and tooth root cannot be loaded independently from each other, it can be shown that the simple empirical method—case depth proportional to module—takes the basic principles of the rolling/sliding contact for tooth flank and of a bending beam for tooth root into good consideration for a wide range of standard gears.

The Loaded Tooth Flank—Some Basic Principles of Contact Stresses

Base model of line contact. In standardized rating of gears according to ISO/DIN, computation of pitting resistance is based on the nominal value of Hertzian pressure at the pitch

point and, especially for helical gears, on the average length of line of contact. For the calculation of the Hertzian pressure, p_H , the meshing of two gear teeth can be represented by an analog model of the meshing of two cylinders under normal load. Important parameters are the radii of curvature for pinion and gear along the length of path of contact and the values of load and pitch line velocity. Characteristic data of material and lubricant have to be introduced. For helical gears, normal unit load is related to minimum total length of line of contact at the appropriate diameter. Figure 1 gives some basic data for two special test gear pairs. The profile of both gear pairs in transverse plane is equal. For the given gear size, a transmission ratio of approximately one leads to a maximum relative radius of curvature in the pitch point C. Both gear pairs have the same face width. The overlap ratio of the helical gear pair is 1.0 for minimizing excitation. As far as the standardized contact stress number σ_{H0}

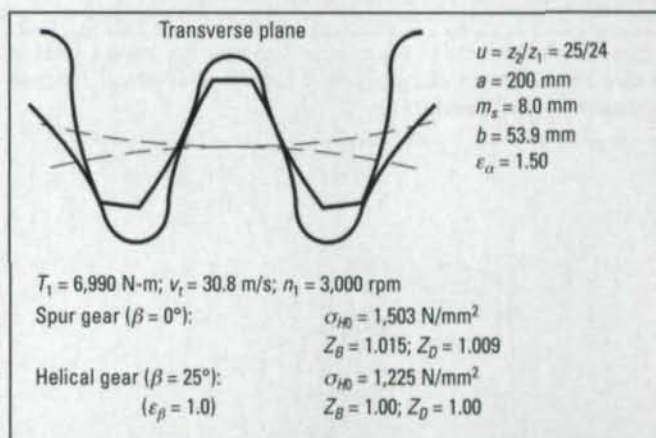


Figure 1—Comparison of a helical and spur gear pair with the same profile in transverse plane.

Dr.-Ing. Thomas Tobie

is a chief engineer at the Gear Research Centre, a part of the Technical University of Munich, located in Germany. A mechanical engineer, he has focused his research work mainly on materials and heat treatment and their influences on the load-carrying capacities of gears, especially regarding pitting and tooth breakage.

Dr.-Ing. Peter Oster

is a chief engineer at the Gear Research Centre and specializes in tribology and load-carrying capacity of gears.

Prof. Dr.-Ing. Bernd-Robert Höhn

is head of the Gear Research Centre. Under his leadership, the centre's main research efforts include examination of load-carrying capacity of gear drives, design of gear geometry and testing of gears.

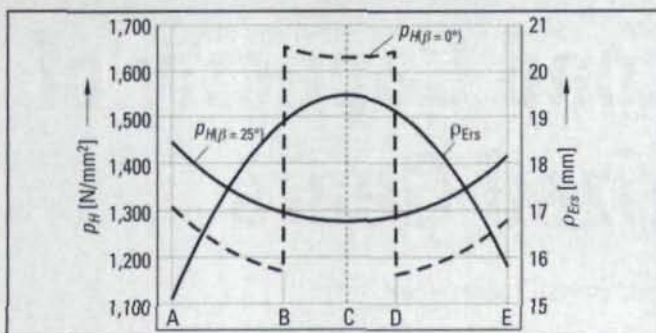


Figure 2—Relative radius of curvature ρ_{Ers} and Hertzian pressure p_H over the line of contact.

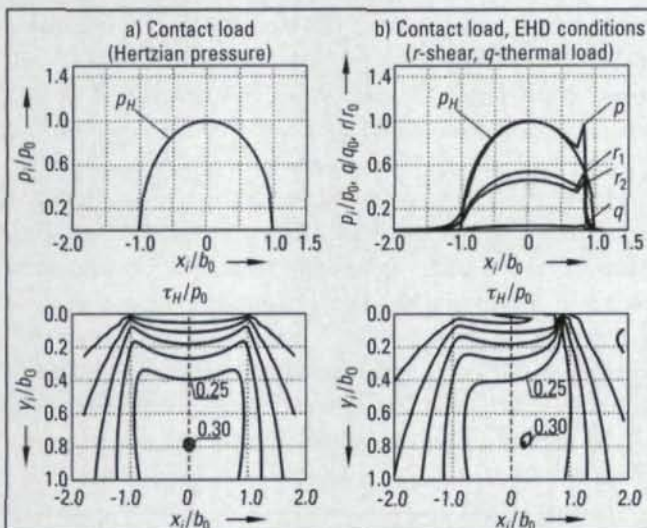


Figure 3—Field of shear stress over depth for the lowest point of single tooth contact of spur pinion regarding elliptical Hertzian pressure (a), EHD pressure (b).

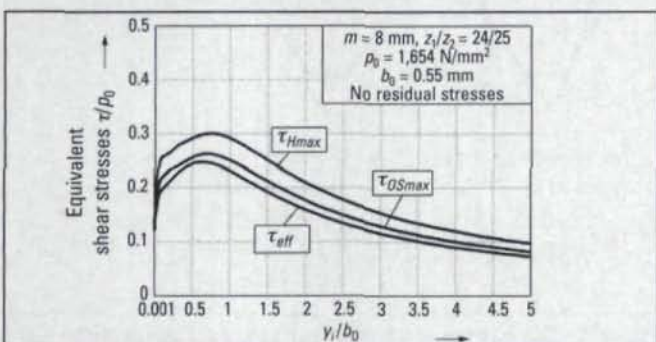


Figure 4—Equivalent shear stresses τ_{Hmax} , τ_{OSmax} and τ_{eff} over depth below surface.

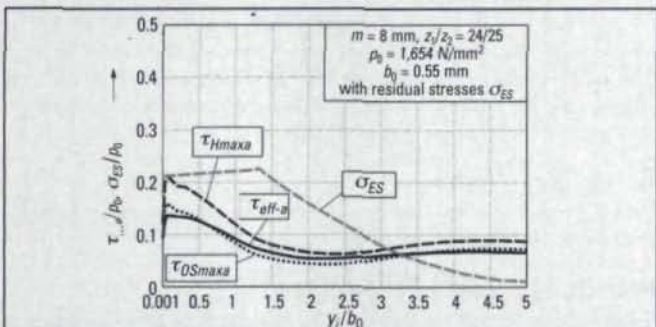


Figure 5—Equivalent shear stress over depth regarding superimposing residual stresses.

according to DIN 3990 (Ref. 2) is concerned, Figure 1 shows that the helical gear is obviously advantageous compared to the geometrically equivalent spur gear. While the helical gear has a constant total length of line of contact, the contact length of the spur gear is significantly characterized by the change of single-to double-tooth contact. Simplifying load distribution, Figure 2 shows the distribution of Hertzian pressure across the path of contact. A is the starting point of mesh at the dedendum flank of the pinion. In the area of small relative radius of curvature ρ_{Ers} and high sliding velocity, the helical gear is loaded with higher Hertzian pressure than the spur gear. The maximum value of Hertzian pressure appears for the spur gear at the lowest point of single tooth contact (point B). With the corresponding local value of load and relative radius of curvature of each contact point, the stress field for line contact can be calculated according to the rules of contact mechanics.

Contact load and contact stresses. For the gear designer, the maximum of the shear stress τ_H or orthogonal shear stress τ_{OS} are two well-known values. Figure 3a shows, for the lowest point of single tooth contact of the spur pinion, the stress field τ_H/p_0 over (material) depth regarding the indicated simple Hertzian pressure. The graphical representation is dimensionless with: p_0 —maximum Hertzian pressure in contact point, y —distance below surface of contact, x —coordinate in contact band or coordinate of time, b_0 —semi width of Hertzian contact band. During teeth meshing, the elliptically distributed Hertzian pressure moves along the length of path of contact. Thus, the load on each single element in the gear volume varies with time, and the direction of the shear stresses changes as load passes through one contact point (rotation by 180° for one mesh).

Therefore, the x -coordinate can be regarded as the time-axis, and consequently, Figure 3 illustrates the variable stress field above time for the chosen contact point. Instead of the dry contact model, actual gears are exposed to a tribological rolling/sliding contact with local friction and varying temperature. Therefore, the normal load induces a tangential component of load as well as a thermal source at the surface. The distribution of tangential load can be assumed as proportional to the distribution of normal pressure, if the average coefficient of friction μ_m is simplified and assumed to be constant.

For the distribution and value of thermally induced stress, the speed conditions of meshing teeth are the most important influence parameters. The lubricant in the tooth contact also affects the pressure distribution. Assuming elastohydrodynamic conditions, the distribution of pressure, film thickness and film condition across the width of the Hertzian contact band can be computed. The distribution of pressure under EHD conditions is primarily influenced by local lubricant viscosity. Important parameters that have an influence on the viscosity at the contact point are value of load, oil temperature and the type of lubricant. Figure 3b shows the local overall loading for EHD contact and the resulting field of shear stress τ_H for the given contact point of the spur gear. It is obvious that friction and an increase in

temperature modify the stress field (for the given gear geometry and load) at and in the near surface-area in a significant way. Additionally, the EHD conditions increase the stress concentration in this area. On the other hand, it is evident that stresses in a depth $y_i > 0.5 \cdot b_0$ are not modified and so values of τ_H are equivalent to the well-known values of loading with pure Hertzian pressure (maximum value of $\tau_H = 0.3 \cdot p_H$ in a depth $y_i = 0.78 \cdot b_0$). The consideration of frictional shear moves the maximum stress in the direction of the end of the Hertzian contact band.

An equivalent stress criterion required for a loaded tooth flank has to take into consideration the multiaxial and variable-with-time stress state of a loaded tooth flank, where the maximum normal and shear stresses occur in different depths below the surface and out of phase.

Equivalent shear stresses. Maximum shear stress criterion (τ_H) and orthogonal shear stress criterion (τ_{OS}), which is proportional to the von Mises equivalent stress, are two basic equivalent stress criteria well known by the gear designer. Figure 4 illustrates for the given loading according to Figure 3b, the values of maximum shear stresses τ_{Hmax} and τ_{OSmax} and the value of the effective shear stress τ_{eff} over depth below surface. By comparing different criteria, it can be noted that τ_{Hmax} as well as τ_{OSmax} are defined as vectors, taking into consideration only the maximum shear stress in a specified plane at a defined point in time. The direction of these stress vectors is variable with time. According to the shear stress intensity method, τ_{eff} is defined as root-mean-square value of all maximum shear stress values $\tau_{y,\varphi}$ in each plane (y,φ) of analysis. Figure 4 points out that for the given gear geometry and load, the profile of the three equivalent stress values is similar, with a maximum value occurring below the surface and the depth and stress value being in the same order of magnitude.

Due to additional residual stresses, the stress distribution shown can be modified quite significantly. Residual stresses are induced by heat treatment and the grinding process. Assuming a biaxial stress state, the normal component of residual stresses is negligible at least in a near-surface region. Therefore, the normal component of residual stresses will be assumed as zero for the following computations.

When superimposing residual stresses, it has to be taken into consideration that residual stresses are more or less constant over time, while stresses induced by external load are variable over time and therefore dynamic components. For the following computations, a variation of the residual stress state due to the running of gears is not considered. The different time profile of load-induced stresses and residual stresses can be considered, if the quasi-static residual stress component—for example, τ_{eff-ES} —is handled as a kind of mean stress. Then the equivalent stresses (indicated by the subscript a , as in τ_{eff-a}) represent a threshold value ($2 \cdot$ amplitude), for example: $\tau_{eff-a} = \tau_{eff} - \tau_{eff-ES}$, where τ_{eff} is the calculated shear stress intensity induced by external load and residual stresses and τ_{eff-ES} is the equivalent



GROUND GEARS – Ten or Ten Thousand

For small to medium quantities of spurs or helicals that have to meet close-tolerance AGMA or DIN specs, our Reishauer grinders and M&M gear analysis systems are the perfect combination.

For Long runs, we offer the unique Liebherr CBN grinding process with full SPC quality control and documentation.

So whether your needs are for ten or tens of thousands, we invite you to join the growing list of INSCO customers who rely on us for consistent quality, reasonable costs, and reliable delivery.



PHONE: 978-448-6368

FAX: 978-448-5155

WEB: inscocorp.com

412 Main Street, Groton, Massachusetts 01450

ISO 9001 Registered

BK

BOURN&KOCH

The Wait is Over.

The Latest In Hobbing Technology Has Arrived.

The 200H/400H Series II from Bourn & Koch... *Simply Incredible.* Call, fax or email us for information on the 200H/400H Series II or one of our many other innovative solutions.

Phone 815/965-4013 Fax 815/965-0019
www.bourn-koch.com bournkoch@worldnet.att.net

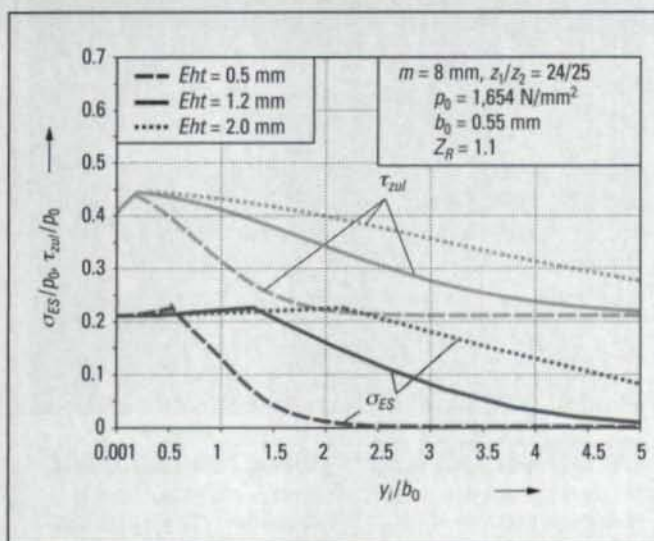


Figure 6—Hardness curve and residual stress profile for different case-depth values.

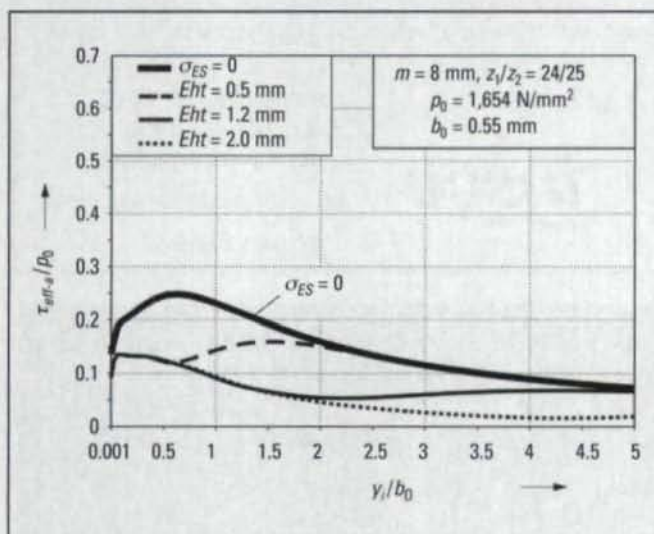


Figure 7—Profiles of τ_{eff-a} without residual stresses and with regard to different residual stresses according to Figure 6.

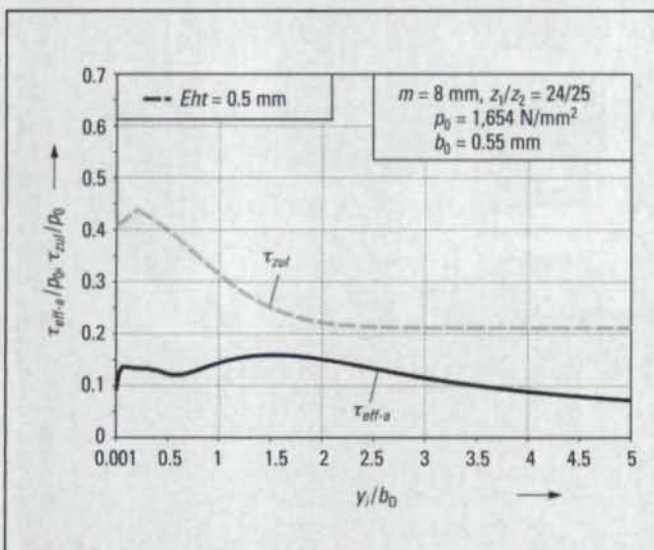


Figure 8—Hardness curve and profile of τ_{eff-a} for a given case depth of 0.5 mm.

shear stress induced by residual stresses only.

For the given example, Figure 5 illustrates the gradient of the equivalent shear stress values over depth considering the shown residual stress state (axial and tangential components of ρ_{ES}). Value and distribution of the given residual stresses agree with measurements in gears of this size and adequate case depth. It is obvious that, with consideration of residual stresses, the equivalent stress levels decrease, in the example in a region $y_i < 4 \cdot b_0$, compared to the stress state without regarding residual stresses. For $y_i > 4 \cdot b_0$, the value of the residual stresses is small in this case, so the influence on load-induced stresses decreases. The different equivalent shear stress values are modified in different ways, but one common effect for all criteria is that the maximum value is now to be found at or very near the surface. Furthermore, it can be seen that after a minimum, the stress values increase again for a depth of $y_i > 2.5 \cdot b_0$. According to Reference 4, the average value of equivalent shear stress in a near-surface area ($y_i < 0.1 \cdot b_0$) is defined as "local near-surface stress," τ_{eff-a} . For the given loading, the values of τ_{eff-a} are reduced by the residual stresses. A decrease of the residual stress value due to running of the gears results in an increase of τ_{eff-a} .

Shear stress/strength gradient for different case depths.

Modifying case depth varies the distance below surface where residual stresses influence the stress state. According to Reference 6, a residual stress profile over depth can be calculated according to a standardized hardness curve. The equations are based on test results. For example, Figure 6 illustrates the influence of variable case depths (Eht) on the gradient of strength (τ_{zul}) and residual stress profile (σ_{ES}) over depth. It is assumed by simplification that the gradient of strength is equivalent to the gradient of hardness (HV) normal to the surface ($\tau_{zul} = c \cdot HV$, $c = 1.0$). Values of surface hardness and core hardness are constant. At and in the near-surface region, the material strength is reduced due to notch effects from surface roughness. Figure 7 shows examples of the gradient of τ_{eff-a} over depth regarding the different residual stress values for different case depths. It can be seen that the stress gradient is modified over different distances below the surface. Especially for a small value of case depth, a second peak value below the surface occurs. At a greater distance below the surface, an increase in case depth leads to a decrease in stress; while in the near-surface area, the stress state is not decreased additionally. Figures 6 and 7 point out that the thickness of the case-carburized layer and thus the case depth modify the strength profile as well as the stress profile over depth significantly.

The variable stress gradient over depth requires a corresponding gradient of strength.

By comparing local stress and local strength over the whole profile, locations of critical stress/strength ratio can be found. In Figure 8, stress and strength profiles are illustrated for the given example with a case depth of 0.5 mm. Note that this case depth is smaller than recommended values in standards. In this case, it can be seen that a section of critical stress/strength ratio, with

respect to minimum safety, is found below the surface at the boundary of the case-core transition. In the case-hardened layer as well as at the surface, the stress/strength ratio is not critical. Figure 9 shows a comparison of stress and strength profile when changing the case depth to 1.2 mm. It is illustrated that stress and strength profile correspond in a much better way over the depth. Maximum stress now occurs near the surface. At a greater distance below the surface, the stress/strength ratio increases, but note that the absolute stress level in these regions is small. However, localized material defects—for example, inclusions—can lead to an increase in stress and initiate a crack below the surface.

Effects of different case-depth values. It was demonstrated that, with consideration of residual stresses, the stress gradient as well as the strength profile over depth are modified with the case-depth value. The depth below the surface of the maximum stress/strength ratio (minimum safety) depends on the correlation of stress and strength profile. Adequate case depth leads to a peak stress value and a critical stress/strength ratio at or just near the surface so that pitting will be initiated in these regions, especially if the special conditions at the surface—for example, notch effects due to surface roughness and decrease of residual stresses due to running of gears—are taken into consideration. These influences modify surface stresses and surface strength. Note that in the examples shown, the different influences on the surface stresses were not taken into special consideration. Smaller values of case depth (or unfavorable residual stresses) can lead to moving the peak value of stress/strength ratio a greater distance below the surface. Thus, gear damage initiated below the surface, especially in regions of critical local stress/strength ratio, may occur. A decrease in load capacity can be imagined. Localized material defects in critically stressed areas increase the risk of damage. On the other hand, lower gear loading can result in lower required case depth.

Thus, for minimizing the risk of tooth flank damage, especially in critical applications, not only conditions at the surface should be regarded. Also, stress and strength profile over depth can be important parameters and should be analyzed by computing a local safety (stress/strength ratio) over depth below the contact. Note that the value of the coefficient c for calculating the material strength— $\tau_{2H} = c \cdot HV$ with $c = 1.0$ —is assumed for simplification and is not based on test results.

The demonstrated theoretical investigations are computed with an EDV-based program system called ROSLCOR, developed, owned and installed by the Technical University of Munich's Gear Research Institute (FZG). Basic principles are summarized in Reference 8.

Application of Test Results in Addition to ISO/DIN Standard

The demonstrated theoretical investigations are in good agreement with some test results run at the FZG for evaluation of the influence of case depth on load capacity. According to Reference 5, an "optimum" case depth guarantees maximum load capacity of tooth flank according to DIN 3990. Smaller val-

SPIRAL BEVEL GEARS (Transmissions)



Spiral & Straight Bevel Gear Manufacturing.
Commercial to aircraft quality gearing.
Spur, helical, splined shafts, internal & external,
shaved & ground gears. Spiral bevel grinding.
Midwest Transmissions & Reducers.
ISO compliant.

MIDWEST GEAR
& TOOL, INC.
12024 E. Nine Mile Road
Warren, MI 48089



CONTACT:
CRAIG D. ROSS
(586) 754-8923
FAX (586) 754-8926

AUTOMATIC INSPECTION

... from the Source

Since 1936 ITW has provided the gear industry with gear inspection devices. Put your trust in the people who invented the process.



High Speed Automatic Functional Tester



Precision Checking Heads

Automatic Functional Gear Inspection In-Line Gages

PRODUCTS AVAILABLE:

- Fully Automatic Machines
- Semi-Automatic Machines
- Manual Double Flank Testers for Coarse and Fine Pitch Gears
- Dimension over Pins/Balls Gage

FEATURES:

- Composite Gaging
- Composite/Center Distance Checks
- Lead/Chord Checks
- SPC Capabilities
- Data Acquisition Screens

For additional information on Gear Burnishing and/or Functional Gear Inspection, visit our website at: www.itwgears.com

ITW Heartland

1205 36th Avenue West
Alexandria, MN 56308 U.S.A.
Ph: (320) 762-8782
Fax: (320) 762-5090
E-mail: itwgears@rea-ep.com

TURNKEY SYSTEMS AVAILABLE.
CUSTOMIZE YOUR APPLICATION:
BURNISHING • WARMER • INSPECTION GAGE.

ues of case depth lead to a decrease in pitting resistance. For the tooth flank, optimum case depth was found as a function of relative radii of curvature. Test results are mainly based on investigations with small gears. Some few test results with larger gears

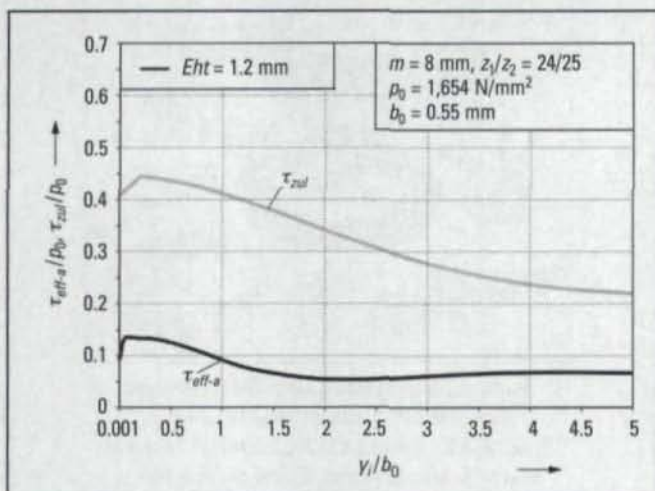


Figure 9—Hardness curve and profile of τ_{eff-a} for a given case depth of 1.2 mm.

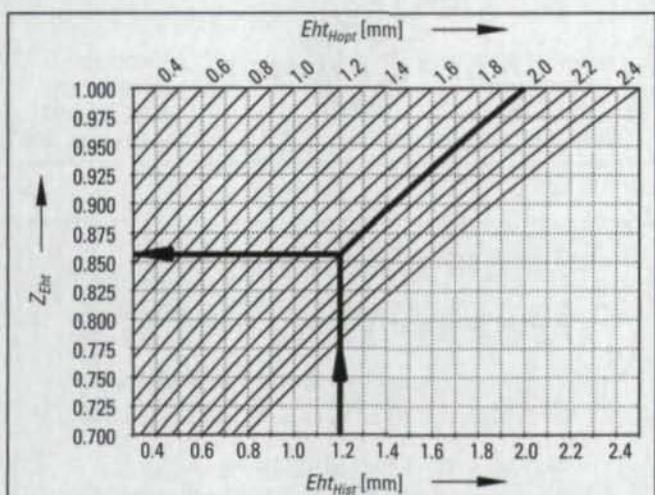


Figure 10—Influence of case depth on permissible contact stress for long life.

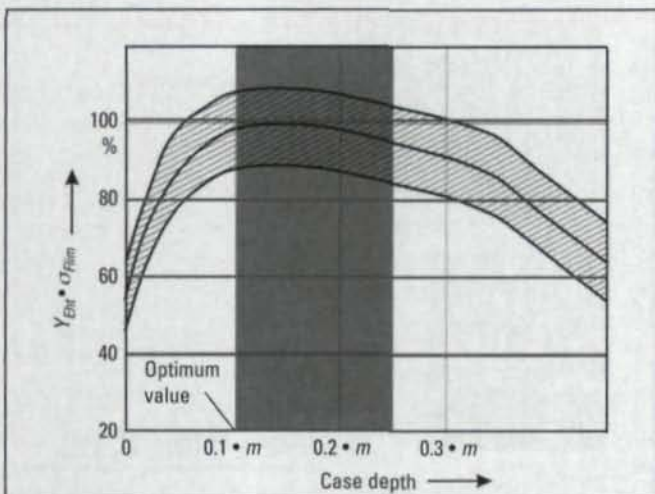


Figure 11—Influence of case depth on tooth root endurance limit (Ref. 7).

($a = 200$ mm) according to Reference 3 confirm these results.

For the tooth root endurance strength, there was also an optimum case depth established, which depends on the module of the gear. Investigations show that smaller or greater values than the optimum case depth decrease the tooth root endurance strength.

The German guideline (Ref. 2), which is based on long practical experience, recommends a case depth of $0.15 \cdot$ normal module, defined as the depth below surface at which the Vickers hardness has dropped to 550 HV, applicable for standard gear sizes. Using this method, the actual load on the gear has not been given special consideration. It is obvious and was demonstrated by theoretical investigations that lightly loaded gears tolerate less case depth than recommended by this rule.

Influence of case depth on contact load capacity. In standardized rating according to ISO/DIN, the allowable stress numbers σ_{Hlim} and σ_{Flim} are valid for a defined optimum case depth. Therefore, an addition to the standard, which is based on the reported test results, is planned to take the influence of variable case depth on load capacity into consideration. For evaluation of the influence of case depth on the permissible endurance contact stress, an influence factor Z_{Eht} (Eq. 1) is defined:

$$Z_{Eht} = \sigma_H \cdot S_H / (\sigma_{Hlim} \cdot Z_W \cdot Z_L \cdot Z_V \cdot Z_R \cdot Z_X) \quad (1)$$

where: σ_H is the actual contact stress number, N/mm^2 ,
 S_H is the required safety factor,
 σ_{Hlim} is the allowable stress number (for optimum case depth), N/mm^2 ,
 $Z_{..}$ are influence factors according to DIN 3990 (Ref. 2).

Within the range $Eht_{Hist} \geq Eht_{Hopt}$: $Z_{Eht} = 1.0$,

Within the range $Eht_{Hist} < Eht_{Hopt}$: Z_{Eht} according to Figure 10 or Equation 2:

$$Z_{Eht} = \sqrt{1 - (170 - 25 \cdot Eht_{Hopt}) \cdot (Eht_{Hopt} - Eht_{Hist}) / 360} \quad (2)$$

where:

Eht_{Hist} is the actual effective case depth (measured at the reference circle),

Eht_{Hopt} is the calculated optimum effective case depth at the reference circle according to Reference 2.

Z_{Eht} is applicable in a range of $0.7 \leq Z_{Eht} \leq 1.0$.

For example:

$$Eht_{Hopt} = 2.0 \text{ mm}, Eht_{Hist} = 1.2 \text{ mm} \\ \rightarrow Z_{Eht} = 0.856.$$

Influence of case depth on bending load capacity. For eval-

uation of the influence of case depth on the tooth root endurance strength, an influence factor Y_{Eht} (Eq. 3) is defined:

$$Y_{Eht} = \sigma_F \cdot S_F / (\sigma_{Flim} \cdot Y_{ST} \cdot Y_{drelT} \cdot Y_{RrelT} \cdot Y_X) \quad (3)$$

where: σ_F is the actual bending stress number, N/mm²,
 S_F is the required safety factor,
 σ_{Flim} is the allowable stress number (for optimum case depth), N/mm²,
 $Y_{..}$ are influence factors according to DIN 3990 (Ref. 2).

Y_{Eht} can be calculated:

• within the range $Eht_{Fist} = 0.025 \dots 0.1 \cdot m_n$:

$$Y_{Eht} = 0.5 + \left(\frac{Eht_{Fist}}{m_n} \right)^{(0.4 - \frac{Eht_{Fist}}{m_n})}$$

• within the range $Eht_{Fist} = 0.1 \dots 0.2 \cdot m_n$:

$$Y_{Eht} = 1.0$$

• within the range $Eht_{Fist} = 0.2 \dots 0.35 \cdot m_n$:

$$Y_{Eht} = 1 - 0.8 \cdot \left(\frac{Eht_{Fist}}{m_n} - 0.2 \right)$$

• where Eht_{Fist} is the actual (measured) effective case depth at the root fillet normal to the 30° tangent,
 Eht_{Fopt} is the calculated optimum effective case depth at the root fillet normal to the 30° tangent according to Figure 11.

For practical application, it can be assumed that:

$$Eht_{Fist} = 0.75 \cdot Eht_{Hst}$$

The influence of case depth on the tooth root endurance limit is also shown in Figure 11. The proposed influence factors can be used in two ways: either for calculation of required case depth as a function of geometry and load or for calculation of the safety factors (load capacity of the gear) for a given case depth not equal to optimum case depth.

Verification of Different Approaches for Determining Case Depth

A gear's tooth flank and tooth root cannot be loaded independently from each other. Thus, an adequate case depth has to consider the basic principles of rolling/sliding contact for tooth flank as well as of a bending beam for tooth root.

In the following, it is demonstrated that the simple empirical method, case depth proportional to module, recommended by the German guideline, takes the different conditions of tooth flank and tooth root into good consideration for a wide range of standard gears. Furthermore, the results are in good agreement with other methods.

Calculation of case depth according to AGMA Standard.

The AGMA standard for gear rating (Ref. 1) recommends a minimum case depth Eht_{min} based on the depth of maximum

shear from contact loading (Eq. 4).

$$Eht_{min} = \frac{\sigma_H \cdot d_{w1} \cdot \sin \alpha_{wt}}{U_H \cdot \cos \beta_b} \cdot \frac{z_2}{z_1 + z_2} = 2.2 \cdot s_{tH} \\ = \frac{2 \cdot \rho_c \cdot \sigma_H}{U_H}; u = \frac{z_2}{z_1} \quad (4)$$

Eht_{min} depends on the actual load on the tooth flank and the geometry of the gear. U_H is a hardening process factor ($U_H = \text{constant} = 66,000 \text{ N/mm}^2$ for grades MQ and ME carburized and hardened). Transforming the given formula, Eht_{min} is proportional to the depth below surface s_{tH} where maximum shear stress τ_{Hmax} occurs, with respect to relative radii of curvature and applied load.

Using the fundamental rating formulas of DIN 3990 (Eqs. 5 and 6) (Ref. 2), some transformations lead to Equation 7.

$$\sigma_H = \sigma_{H0} \cdot \sqrt{K_A K_V K_{H\alpha} K_{H\beta}} \leq \sigma_{HP} = \frac{\sigma_{Hlim}}{S_{Hmin}} \cdot Z_W Z_L Z_R Z_X Z_Y \\ \sigma_{H0} = Z_H Z_E Z_B Z_c Z_\beta \cdot \sqrt{\frac{F_t}{d_1 b} \frac{u+1}{u}} = Z_H Z_E Z_B Z_c Z_\beta \cdot \sqrt{\frac{F_t \cos \beta}{b z_1 m_n u} \frac{u+1}{u}} \\ \Rightarrow \sigma_{H0} = Z_H Z_E Z_B Z_c Z_\beta \cdot \sqrt{\frac{F_t \cos \beta}{b z_1 m_n u} \frac{u+1}{u}} = \frac{\sigma_{Hlim}}{S_H} \cdot \frac{Z_W Z_L Z_R Z_X Z_Y}{\sqrt{K_A K_V K_{H\alpha} K_{H\beta}}} \quad (5)$$

$$\sigma_F = \sigma_{F0} \cdot K_A K_V K_{F\alpha} K_{F\beta} \leq \sigma_{FP} = \frac{2 \sigma_{Flim}}{S_{Fmin}} \cdot Y_X Y_{drelT} Y_{RrelT} \\ \Rightarrow \sigma_{F0} = \frac{F_t}{b m_n} \cdot Y_{FS} Y_e Y_\beta = \frac{2 \sigma_{Flim}}{S_F} \cdot \frac{Y_X Y_{drelT} Y_{RrelT}}{K_A K_V K_{F\alpha} K_{F\beta}} \quad (6)$$

$\frac{\sigma_{F0}}{\sigma_{H0}} = \text{function of } z_1$ (z_1 – number of pinion teeth):

$$z_1 = 2 \cdot \frac{S_H^2}{S_F} \cdot \frac{\sigma_{Flim}}{\sigma_{Hlim}^2} \cdot \frac{u+1}{u} \cdot \cos \beta \cdot \frac{(Z_H Z_E Z_B Z_c Z_\beta)^2}{(Z_W Z_L Z_R Z_X Z_Y)^2} \cdot \frac{Y_X Y_{drelT} Y_{RrelT}}{Y_{FS} Y_e Y_\beta} \cdot \frac{K_A K_V K_{H\alpha} K_{H\beta}}{K_A K_V K_{F\alpha} K_{F\beta}} \quad (7)$$

Application of Equations 4 and 7 results in Equation 8, in which Eht_{min} is proportional to various influence factors, to the actual safety factors, and to the gear module:

$$Eht_{min} = \frac{2}{U_H} \cdot \frac{(Z_H Z_E Z_B Z_c Z_\beta)^2}{(Z_W Z_L Z_R Z_X Z_Y)} \cdot \frac{Y_X Y_{drelT} Y_{RrelT}}{Y_{FS} Y_e Y_\beta} \cdot \frac{K_A K_V K_{H\beta} K_{H\alpha}}{K_A K_V K_{F\alpha} K_{F\beta}} \cdot \frac{\sin \alpha_{wt}}{\cos \beta_b} \cdot \frac{\cos \alpha_t}{\cos \alpha_{wt}} \cdot \frac{\sigma_{Flim}}{\sigma_{Hlim}} \cdot \frac{S_H}{S_F} \cdot m_n \quad (8)$$

The given equations are based on mathematically exact transformations and therefore can be used for all types of involute spur and helical gears.

Assuming some simplifications and reasonable values for the influencing factors, applicable for standard gear sizes and standard gear applications, Equation 8 can be written as:

$$Eht_{min} = 0.16 \cdot \frac{S_H}{S_F} \cdot m_n \quad (9)$$

Comparison of the different approaches for determining case depth. From Equation 9, it is obvious that for standard gear sizes, the different methods for calculating case depth according to DIN 3990 ($Eht_{Hopt} = 0.15 \cdot m_n$) and AGMA lead to very close results, if optimum load capacity is required (safety factors near 1).

For lightly loaded gears, Equation 9 tolerates less case depth ($S_F \sim \sqrt{S_H}$, $S_F > S_H > 1$!).

According to the German guideline (Ref. 2), the actual load has not been given special consideration, so optimum case depth for optimum load capacity is always obtained. Introduction of the defined influencing factors Z_{Eht} and Y_{Eht} into the DIN standard takes actual stress conditions into consideration. This means that, for lightly loaded gears, the required case depth can be reduced compared to the recommended optimum case depth. Thus, for a wide range of standard gears, the two methods are applicable, especially if the actual safety factors S_H and S_F (actual load) are used for calculation. Especially for large gears, the maximum allowable stress numbers are often not used due to safety aspects.

Note that for some special gears, calculated values of case depth will differ because Eht_{min} depends on the gear geometry in question and on the real contact stress number σ_H . For critical gearing, detailed studies should be made according to the section "The Loaded Tooth Flank—Some Basic Principles of Contact Stresses."

Conclusion

The allowable stress numbers in standardized rating of gears are valid for normal (optimum) case depth. It is known that especially small case depth values can reduce contact and bending load capacity. In theoretical investigations, it was shown that the loading of tooth flank by Hertzian pressure and tribological parameters induces a stress field in the material, which is variable over depth and can be calculated according to the rules of contact mechanics.

Application of different equivalent shear stress criteria shows that residual stresses can modify the stress state significantly. It was demonstrated that variation of case depth influences the stress gradient as well as the strength gradient over depth. By analyzing the local stress/strength ratio over the tooth profile and depth, a local safety factor can be defined. The depth below surface where the maximum stress/strength ratio occurs depends on the relation of the stress and the strength profile. Adequate case depth leads to a peak value of the stress/strength ratio at or just near the surface. Smaller values of case depth can lead to a relocation of the maximum value of stress/strength ratio at a greater distance below the surface. That relocation may lead to gear damage that initiates below surface. Lower gear loading can result in lower required case depth.

An addition to the ISO/DIN standard is proposed in which the influence of different case depths on load capacity can be

taken into consideration.

It was shown that the simple empirical method—case depth proportional to module—recommended by the German guideline (Ref. 2), takes the different conditions of tooth flank and tooth root into good consideration for a wide range of standard gears. Using the proposed influence factors Z_{Eht} and Y_{Eht} , the results for calculated case depth according to the empirical method are in good agreement with other methods (Ref. 1) for calculation of required case depth with consideration of actual load. \odot

References

1. American National Standards Institute, ANSI/AGMA 2001-C95 (1995), *Fundamental Rating Factors and Calculation Methods for Involute Spur and Helical Gear Teeth*.
2. German National Standards Institute, DIN 3990 part 1...5 (1987), *Calculation of Load Capacity of Involute Gears*. (In German.)
3. Forschungsvereinigung Antriebstechnik e.V. (FVA). *Basic Investigations for Evaluation of Adequate Case Depth for Rolling/Sliding Contact and Bending Load—Additional Tests for Evaluation of Influence of Gear Size on Case-Hardened Gears made from 16 MnCr 5*, FVA Report No. 223 (1986). (In German.)
4. Höhn, B.-R. and P. Oster, "The Gear Flank Contact—An Elasto-Hydrodynamic Rolling/Sliding Contact," VDI-Report No. 1207 (1995), pp. 93–106. (In German.)
5. Käser, W. *Contributing Factors to Pitting in Case-Hardened Gears: Influence of Case Depth and Lubrication on the Flank Load Carrying Capacity*. Dissertation, TU München (1977). (In German.)
6. Lang, O.-R. "Calculation and Dimensioning of Induction Hardened Components," *Induction-Hardening*, Report of AWT-Congress, Darmstadt (1988), pp. 332–348. (In German.)
7. Niemann, G. and H. Winter, *Machine Elements*, Volume 2, Springer-Verlag (1983). (In German.)
8. Oster, P. *The Stress on Gear Flanks Considering Elasto-Hydrodynamic Conditions*, Dissertation, TU München (1982). (In German.)

This paper was presented at the 4th World Congress on Gearing and Power Transmission, Paris, March 1999 and in *Organi di Trasmissione*, February 2000.

Tell Us What You Think . . .

Visit www.geartechnology.com to

- Rate this article
- Request more information
- Contact the author or companies mentioned
- Make a suggestion

Or call (847) 437-6604 to talk to one of our editors!